

THE POSSIBILITY OF UTILIZATION OF THE EQUATORIAL ATMOSPHERE RADAR (EAR) ON STUDY THE EFFECTS OF GRAVITY WAVES ON A CORRUGATED STRUCTURE OF REFLECTION SURFACE

Eddy Hennawan
Peneliti Pusat Pemanfaatan Sains Atmosfer dan Iklim, LAPAN

ABSTRACT

We have introduced a new Equatorial Atmosphere Radar (EAR), a collaboration project between Research Institute for Sustainable Humanosphere (RISH), Kyoto University, Japan and the Indonesian National Institute of Aeronautics and Space (LAPAN) at Kototabang, Bukittinggi, West Sumatera. This radar is mainly concerned to observe winds and turbulence in the troposphere and lower stratosphere with a good time and spatial height resolution. Numerous study or research programs with the EAR are still developing. In this paper, one possibility an application of EAR on study effects of gravity waves on a corrugated reflection surface is discussed. For the reference, we investigated the azimuth angle variations of clear air echoes in the troposphere and lower stratosphere by using the MU (Middle and Upper atmosphere) radar in Shigaraki, Japan ($34^{\circ}51'$; $136^{\circ}06'E$). We used a data set collected on November 4-5, 1986 by steering the antenna beam into 12 oblique positions at the same zenith angle of 6° and the azimuth angle being changed every 30° . We have detected considerable amplitudes in the azimuth angle variations of echo power, which was continuous along altitude. We also found time evolution of the azimuth angle variations of echo power. The observed azimuth angle variations of echo power suggest that the reflection surface is affected by propagating gravity wave. As a preliminary result, we present characteristics of zonal and meridional wind velocity observed with EAR on May 24-25, 2001 over Kototabang after validated by GPS (Global Position Satellite) radiosonde. The long-term observations of the variations of meridional wind velocity from September to December 2001 as one of the most important parameter needed to explain the mechanism of gravity waves is also discussed.

ABSTRAK

Kami telah memperkenalkan suatu radar baru bernama Radar Atmosfer Katulistiwa (RAK) yang merupakan proyek kerja sama antara *Research Institute for Sustainable Humanosphere* (RISH), Universitas Kyoto, Jepang dengan Lembaga Penerbangan dan Antariksa Nasional (LAPAN) di Kototabang, Bukittinggi, Sumatera Barat. Perhatian utama radar ini adalah untuk meneliti perilaku angin dan turbulensi yang terjadi di lapisan troposfer

dan bawah stratosfer dengan resolusi waktu dan ketinggian yang relatif sangat singkat (masing-masing dalam orde menit dan meter). Beberapa program studi atau penelitian dengan menggunakan data RAK hingga kini terus dikembangkan. Pada makalah ini, ditinjau salah satu kemungkinan pemanfaatan data RAK pada studi pengaruh gelombang gravitasi pada struktur lapisan pantul yang bergelombang (*corrugated layer*) didiskusikan. Sebagai bahan acuannya, kami mengkaji variasi sudut azimuth dari pada *clear air echo* pada lapisan troposfer dan stratosfer bawah dengan menggunakan data MU (Middle and Upper atmosphere) radar yang ada di Shigaraki (340511-1); ISeooeBT), Jepang. Kami menggunakan data tanggal 4-5 November 1986 yang menggunakan *steering antenna* (antenna putar) sebanyak 12 posisi *oblique* (membentuk sudut 6 derajat off-vertikal) yang diputar setiap 30 derajat. Kami juga telah mendeteksi kemungkinan peranan variasi amplitude sudut azimuth dari pada *echo power* yang kontinu terhadap ketinggian. Kami juga menemukan adanya evolusi waktu dari pada variasi sudut azimuth *echo power*. Hasil pengukuran variasi sudut azimuth *echo power* menyarankan bahwa lapisan permukaan pantul dipengaruhi oleh gelombang gravitasi. Sebagai hasil awal, kami tunjukkan karakteristik angin zonal dan meridional hasil pengukuran RAK pada 24-25 Mei 2001 di atas Kototabang sc telah data terse but divalidasi dengan data GPS [*Global Position Satellite*] radiosonde. Pengamatan jangka panjang tentang variasi angin meridional periode September hingga Desember 2001 sebagai salah satu komponen penting dalam menjelaskan mekanisme terjadinya gelombang gravitasi juga didiskusikan.

Kata kunci: *Radar Atmosfer Katulistiwa (RAK), gelombang gravitasi, angin zonal, angin meridional*

1 INTRODUCTION

For the study of the equatorial atmosphere, especially over Indonesian region, the Equatorial Atmosphere Radar (EAR) has been constructed at Kototabang, Bukittinggi, West Sumatera, Indonesia. It is large Doppler monostatic radar built for atmospheric observation. It was completed in March 2001 and has been operating since June 26, 2001 until now. This radar is a collaboration project between Research Institute for Sustainable Humanosphere (RISH) of Kyoto University, Japan and the Indonesian National Institute of Aeronautics and Space (LAPAN).

As we know, a few most important environmental phenomena such as ENSO (El-Nino and Southern Oscillation), seawater exchanges between the Pacific Ocean and the Indian Ocean through the channels and straits of the neighboring water of Indonesia, the Monsoon changes between the Asian Continent and the Indian Ocean, and biomass burning occur in the South-East Asian region. These phenomena cause the inter-annual variations of the Monsoon and rainy season, including frequent and large-scale floods, drought and air pollution there, by which development of South-East Asian countries have been seriously affected.

The western Pacific region called the Indonesian Archipelago is the center of the intense atmospheric motions and global atmospheric changes. However, the mechanisms of the atmospheric changes and fluctuations have not yet been made clear due to the sparseness of observation data in that region. Recent uncontrolled fires in Indonesia demonstrate that the local impact to the atmosphere is not yet limited to the Indonesian area, but easily expands to its neighboring countries.

It is now strongly requested that we evolve studies of the equatorial atmosphere in large spectrum. The mechanisms that cause atmospheric changes are considered to have a hierarchical structure or multiple structures, which requires observing the atmosphere with different horizontal scales as shown in Figure 1-1.

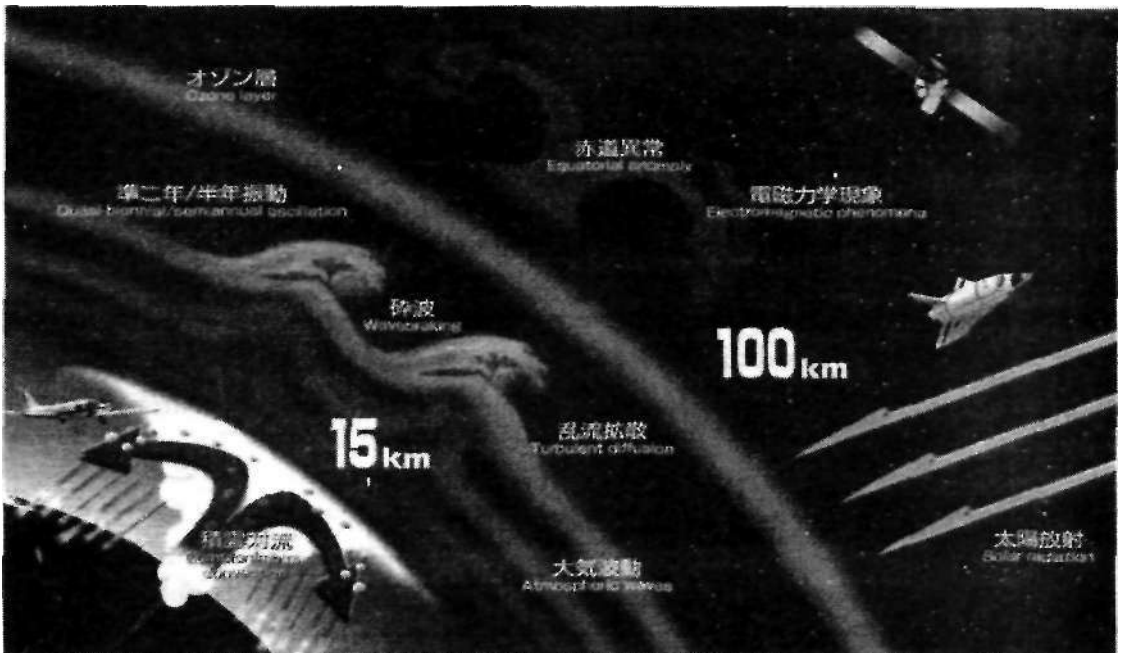


Figure 1-1: Dynamical atmospheric processes in the equatorial atmosphere, especially over Indonesia ([http://www.rish.kyoto-u.ac.jp/cpea/CPEA-Eng-Frame, htm](http://www.rish.kyoto-u.ac.jp/cpea/CPEA-Eng-Frame.htm))

Recently, efforts for networking atmospheric radars which are reputable for its reliable and continuous operation have been initiated by scientist from the US, Australia and Japan. One of such networks is the Trans-Pacific Network operated by LAPAN and the US National Oceanic and Atmospheric Administration (NOAA). It consists of five radars lining up along the equator from Peru in South America to Biak Indonesia. A couple of similar, but less sensitive radars is also operating in India and Thailand. However, its coverage is far from the entire Southeast Asian region, especially in the Indonesian Archipelago. It is expected that effective data will be available for elucidating the mechanisms from the network, if a few more radars will be established there additionally to the present radar network.

In 1992, RASC started continues operation of two radars, a Boundary Layer Radar (BLR) and Meteor Wind Radar (MWR) in PUSPIPTEK under the collaboration with BPPT. An MF (Middle Frequency) radar in Pontianak was established in 1995 by the collaboration with LAPAN and the University of Adelaide (Australia). The other BLR was installed in the GAW (Global Atmospheric Watch) facility in 1998, which was located just next to the site of the EAR. The location of the EAR and related facilities of radar in Indonesia can be seen in Figure 1-2.



Figure 1-2: The location of the EAR and related other facilities (<http://www.rish.kyoto-u.ac.jp/cpea/CPEA-Eng-Frame.htm>)

2 THE SPECIFICATIONS OF EAR

The EAR has a circular antenna array of approximately 110 m in diameter, which consist of 560 three-element yagi as shown in Figure 2-1.

It is an active phased array system with each yagi driven by a solid-state transceiver module. This system configuration makes it possible to direct the antenna beam by electronic control up to 5000 times per second. The EAR transmits an intense radio wave of 47 MHz to the sky, and receives extremely weak echoes scattered back by atmospheric turbulence. It can observe winds and turbulence in the altitude range from 1.5 km to 20 km (troposphere and

lower stratosphere). It can also observe echoes from ionospheric irregularities at heights more than 90 km. The explanations more detail is presented at Table 2-1.

Numerous study programs with the EAR are developing now. One of them is the possibility an application of EAR on study the effects of gravity waves on a corrugated structure of reflection surface, especially in the troposphere and lower stratosphere. For the reference, we are interest to review first the basic concept of this study observed with the MU (Middle and Upper atmosphere) radar at Shigaraki, Japan. Then, we try to apply it on the EAR observations.

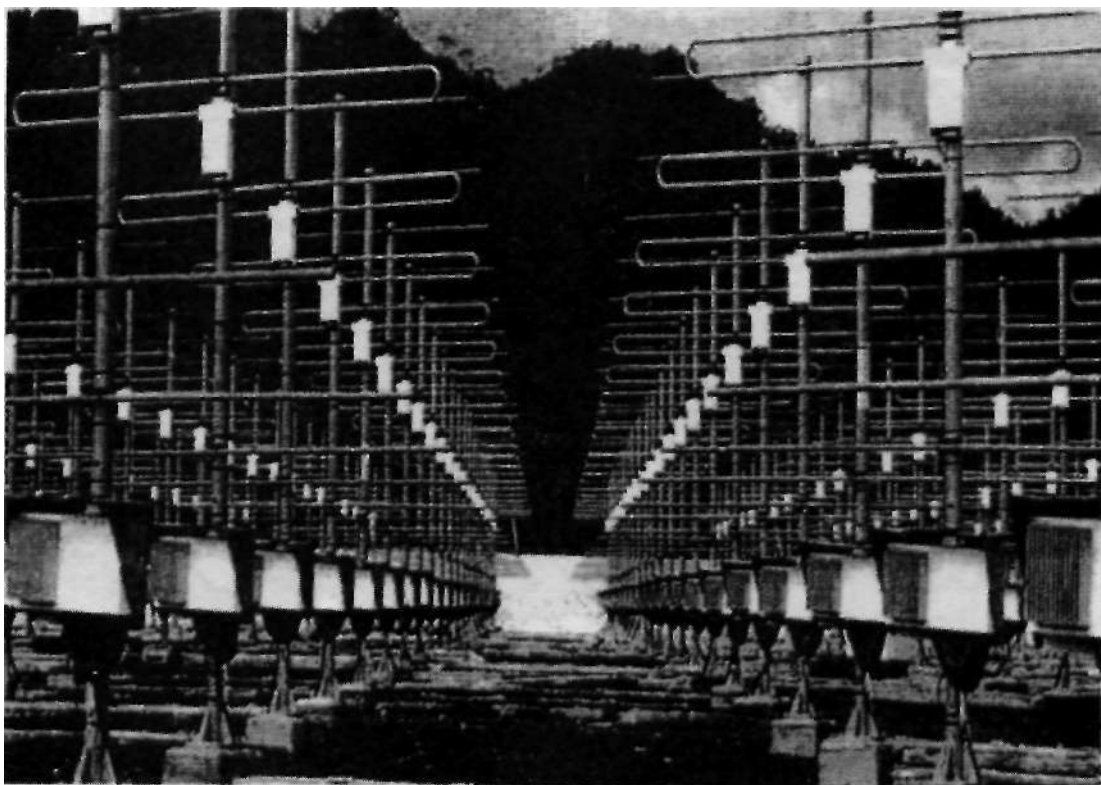


Figure 2-1: The antenna field of the EAR (<http://www.rish.kyoto-.ac.jp/cpea/CPEA-Eng-Frame.htm>)

Table 2-1: THE SPECIFICATIONS OF THE EAR

Location	100.32° E ; 0.20° S ; ± 865 MSL (Mean Sea Level)
Frequency	47 MHz
Output power	100 kW (peak envelope)
Antenna system	Quasi-circular active phased array (H0m-diamter, 560 three-element yagi)
Beam width	3.4° (-3dB, One-way)
Beam direction	Anywhere (within 30° zenith angles)
Observation range	1.5 - 20 km (Atmospheric turbulence) > 90 km (Ionospheric irregularity)

3 THE BASIC CONCEPT EFFECTS OF GRAVITY WAVES

Study of azimuth angle variations of echo power in the troposphere and lower stratosphere has been done by Tsuda *et al.* (1997). They reported that in the troposphere the azimuth angle variations of echo power is generally small, but becomes large in the lower stratosphere. This large azimuth variations seem to be associated with the aspect sensitivity of echo power, suggesting that the reflection surface is corrugated probably because the effect of gravity waves.

It is now widely accepted that meso-scale fluctuations of wind velocity and temperature in the middle atmosphere are caused by atmospheric gravity waves, which are mainly excited in the lower atmosphere due to, for example, the unstable behavior of and/or the interaction of the topography with a jet stream, and various meteorological disturbances such as fronts, typhoon, thunderstorms and cumulonimbus convections.

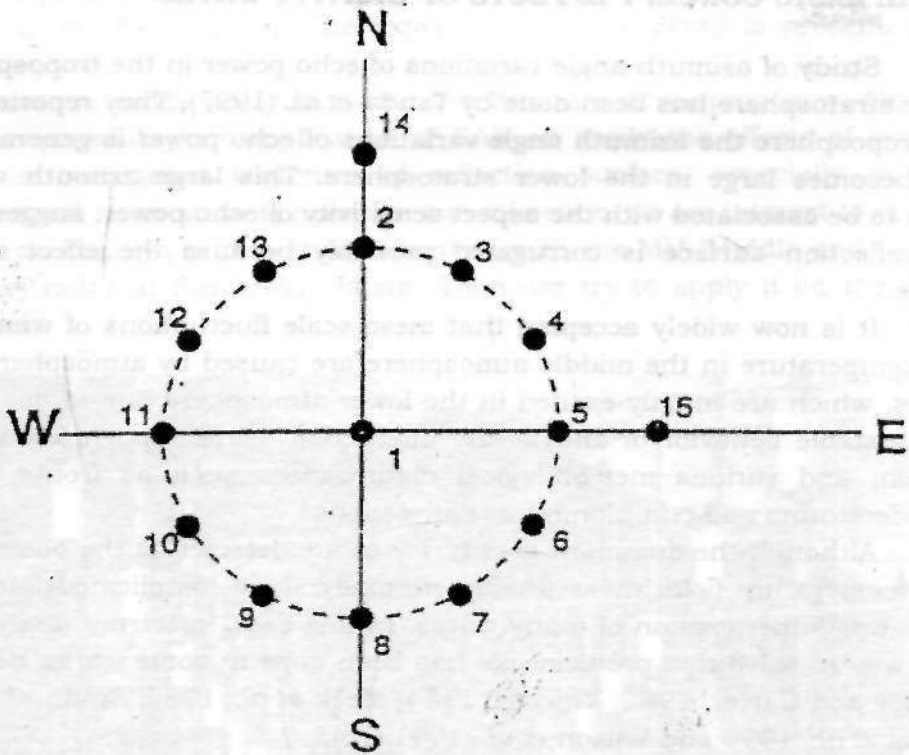
Although the dominant gravity waves are detected in the observed wind and temperature field, these profiles normally show complicated fluctuations, indicating superposition of many waves. In this case, spectrum analysis is the best way to solve this problem like has been done in some works before (*e.g.*, Balsley and Carter, 1982; Vincent, 1984; Meek *et al.*, 1985; Smith *et al.*, 1985; Tsuda *et al.*, 1990 and Wilson *etal.*, 1991a, b).

Tsuda *et al.* (1988) found a correlation between the gravity wave activity and the vertical structure of the reflection echoes from the MU (Middle and Upper atmosphere) radar observations, especially in the lower stratosphere, where specular reflection is dominant. Reflection echo power is proportional to the square of mean gradient of refractive index, M , which includes Brunt Vaisala frequency squared, N^2 . Since N^2 is defined by the vertical derivative of potential temperature with the altitude, A_f includes temperature fluctuations due to gravity waves.

It is expected therefore that horizontal structure of a reflection surface be modified by gravity waves. If a reflection layer passes over the radar, following the motion of gravity waves, reflection echoes may not be detected only in the vertical direction, but they can be received from any direction perpendicular to the corrugated surface.

4 EXPERIMENTAL SETUP

We review firstly here a case study by Tsuda *et al.* (1997) using data collected for about 22 hours on November 4-5, 1986. Note that the data were sampled every 150 m at 6-16 km. During this observation 523 vertical and oblique echo power profiles were obtained. Antenna beam was directed to vertical and 12 oblique beam positions at 6° off the zenith by changing the azimuth every 30° . While other two beam directions were also used for the reference. Figure 4-1 shows antenna beam positions.



1 (0 , 0)	9 (210, 6)
2 (0 , 6)	10 (240, 6)
3 (30 , 6)	11 (270, 6)
4 (60 , 6)	12 (300, 6)
5 (90 , 6)	13 (330, 6)
6 (120, 6)	14 (0 , 10)
7 (150, 6)	15 (90 , 10)
8 (180, 6)	

Figure 4-1: The beam directions for observations of the azimuth angle dependence of the echo power on November 4-5, 1986. Full circles denote the beam directions (after Tsuda *et al*, 1997)

While, Figure 4-2 shows a time-height section of signal-to-noise ratio (SNR) for vertical echoes averaged for 6 min. In later sections we concentrate on observation during 3:01-5:27 LT on November 5, 1986 when corrugated reflection layers were clearly recognized.

Normalized Signal to Noise Ratio (Vortical Beam)

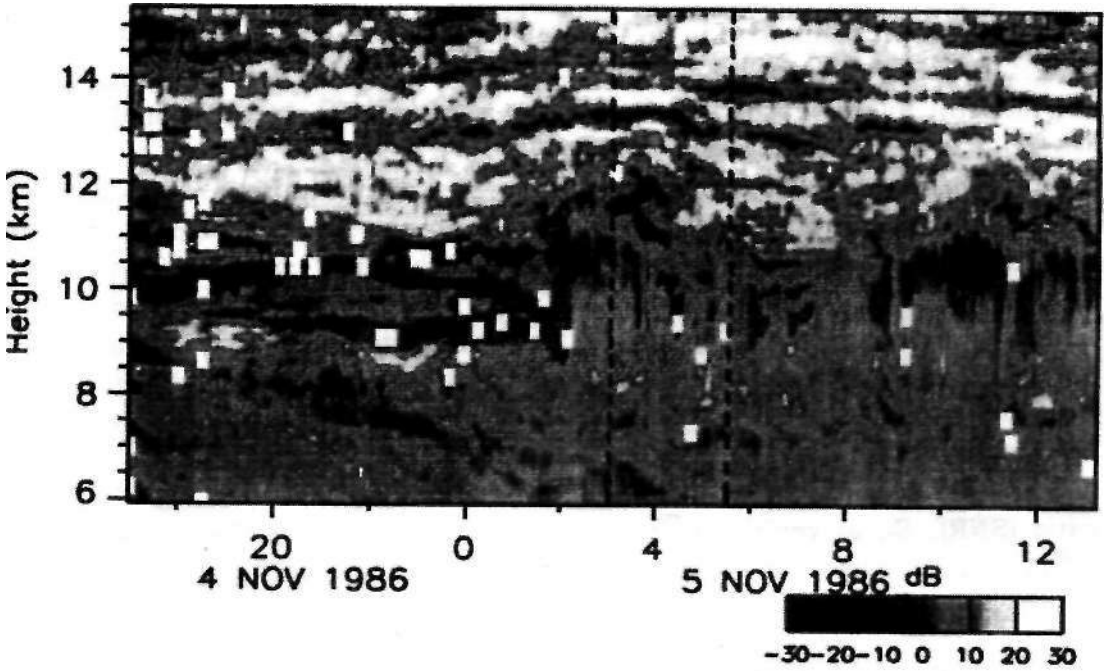


Figure 4-2: The normalized signal-to-noise ratio (SNR) for vertical beam direction on November 4-5, 1986

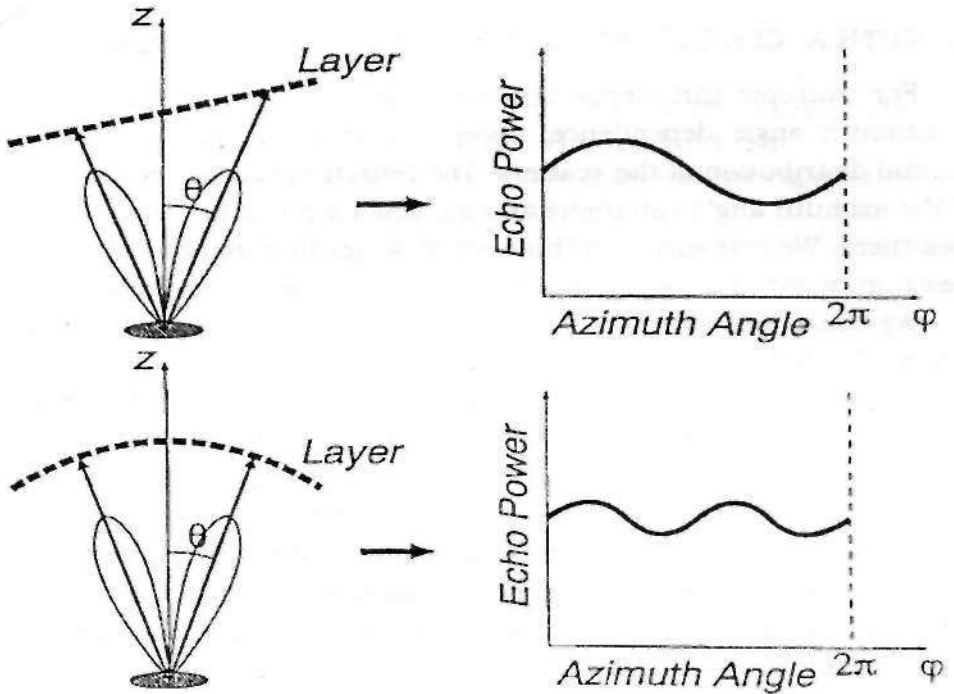


Figure 4-3: The schematic idea of the reflection echoes from linearly tilted (top) and corrugated layers (bottom) (after Tsuda. et al, 1997)

By assuming a titled flat layer in Figure 4-3, the azimuth angle variation of echo power shows single maximum and minimum in one full cycle of azimuth angle. This condition may be caused by a large-scale thermal structure of the troposphere or by a wave with a very long horizontal wavelength. In this case, we can see that echo power is proportional to $\sin\theta$, where θ is the azimuth angle.

When the reflection surface layer has a curvature as illustrated in Figure 4-3, the azimuth angle variation of echo power could have two maxima and two minima, which is called a "double humped structure". It can be derived that the azimuth variation of echo power is proportional to $\sin\theta$ or $\sin 2\theta$, depending on the phase of the corrugated reflection surface. This condition can be caused by the effects of vertical displacement due to gravity waves (Tsuda *et al*, 1997). That is, vertical motions due to gravity waves could modify the shape of a reflection layer, producing a wavy structure.

In later sections, we use for convenience the normalized signal-to-noise ratio (SNR), S_θ , at zenith angle θ , after compensating for the range-squared effect and decrease of the effective antenna area as follows (Tsuda *et al*, 1997):

$$S_\theta = (1 / \cos^2\theta)(P_e/P_N)(r/10\text{km})^2 \dots\dots\dots (4-1)$$

where P_e , P_N and r are the echo power, the noise level and the range in km, respectively. Note that, S_θ is the normalized to the altitude of 10 km. Thus, the power reflection coefficient, r_{jref} , becomes proportional to S_θ .

5 AZIMUTH ANGLE DEPENDENCE OF REFLECTION ECHOES

For isotropic turbulence scattering, the echo power does not seem to have azimuth angle dependence, except for that due to an inhomogeneous horizontal distribution of the scatters. The reflection echoes are not expected to have the azimuth angle variations as well, when a horizontal stratified flat layer causes them. We investigate in this section azimuth variations of the reflection echoes that might arise because of the modified reflection surface.

We present in Figure 5-1 an example of profiles for S_θ , S_6 and S_e/S_θ on November 5, 1986 from 09:00 to 09:02 LT between 6 and 15.5 km. The center and right panels simultaneously illustrate S_6 and S_e/S_θ in 12 beam directions at the same zenith angle of 6° from different azimuth angles. These profiles were roughly similar with each other, but their fine structures are fairly different particularly above 12 km. Larger azimuth variations of S_6 were associated with large aspect sensitivity as shown in the right panel in Figure 5-1. which suggests that the large azimuth variations of S_e are closely related to a reflection echo. On the other hand, the echo power did not vary greatly in different azimuth directions, where isotropic scattering from a horizontal homogeneous layer is dominant.

PROFILE OF VERTICAL AND OBLIQUE ECHO POWER AT 6°

(5-NOVEMBER-1986 ; 09:00:28 - 09:02:45 LT)

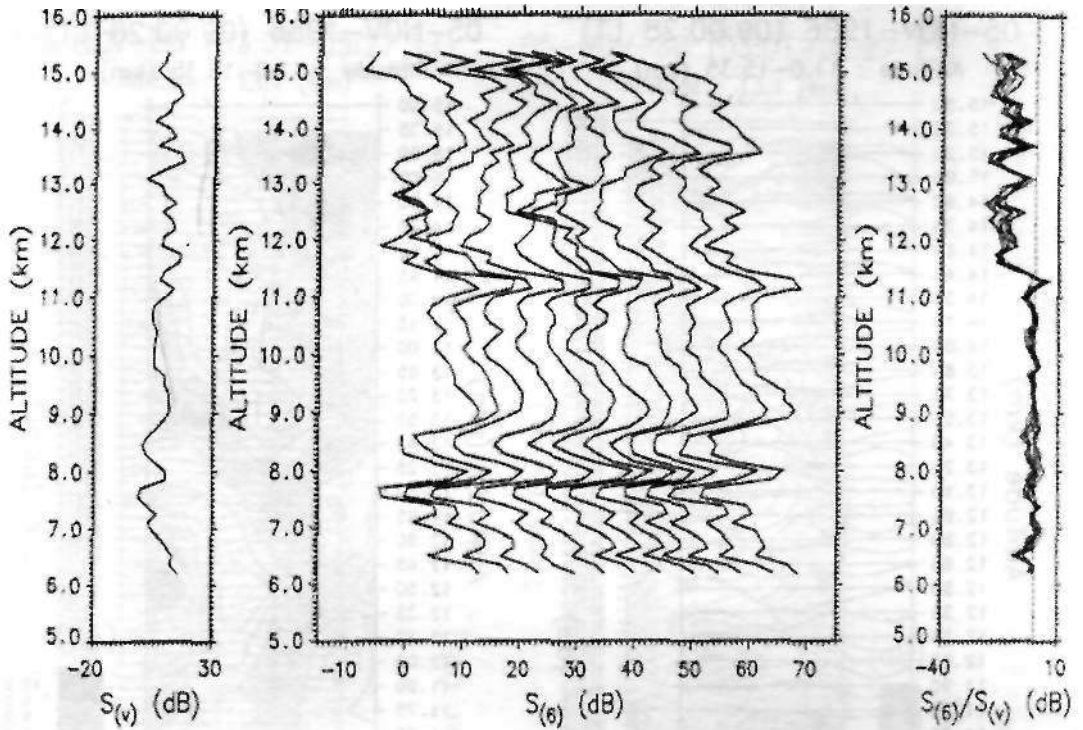
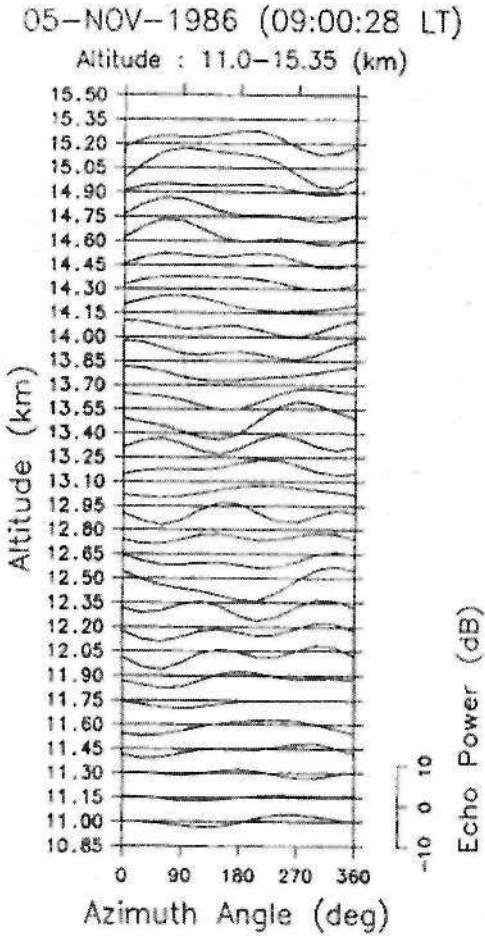


Figure 5-1: The profile of the vertical echo power, S_v (left) observed on the MU radar observations on November 5, 1986 from 09:00:28 to 09:02:45 LT. Twelve profiles of oblique echo power at 6°, S_6 are plotted in the center panel, shifting every 5 dB. The ratio of the vertical to oblique echo power, S_6/S_v is simultaneously shown in the right panel

Figure 5-2 (a) and (b) show height variations of azimuth angle dependence of the echo power for the MU radar observation on November 5, 1986 at 09:00:28 LT after subtracting to the mean value at each height. It is clear that azimuth variations of echo power existed with one or two sinusoidal cycles in 360° azimuth angle. In particular, from 12.5 to 13.40 km, the ratio of the maximum to minimum echo power sometimes exceeded 10 dB. Note that the variations were continuous in altitude, and they were well correlated between adjacent heights for a fairly large height range. Therefore, it is suggested that underlying physical mechanism also extended in the vertical direction, which can be realized, for instance, by a gravity wave.

(a)



(b)

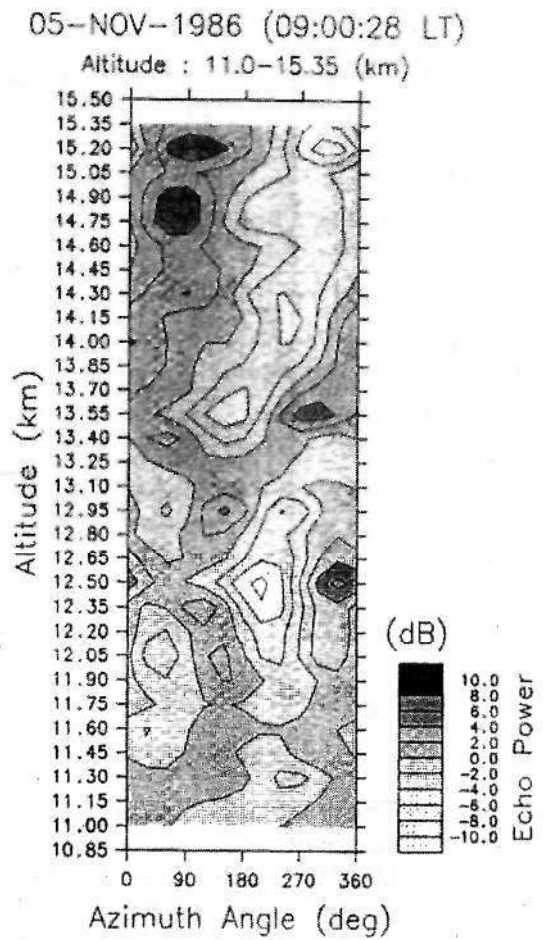


Figure 5-2: Azimuth angle variations of the echo power observed on November 5, 1986, illustrated at height (a), and (b) a contour plot

Figure 5-3 (a) shows time evolution of the azimuth angle dependence of echo power at 13.10 km altitude after subtracting the mean time between 03:01 and 05:27 LT on November 5, 1986. Again, we can see a clear azimuth variation of echo power, with a single and double humped structures, especially from 03:17-03:49 LT to 04:12-04:49 LT. A contour map in Figure 5-3. (b) also demonstrates continuous time changes more clearly.

We applied a least square fitting of harmonic functions to the azimuth angle variations of the echo power as :

$$P(\theta) = A_{360} \sin(\theta + \theta_{360}) + A_{180} \sin(2(\theta + \theta_{180})) \dots\dots\dots (5-1)$$

where A and 0 are amplitude and phase of the azimuth angle variations of the echo power. In particular, θ_{360} and θ_{180} are an initial phase.

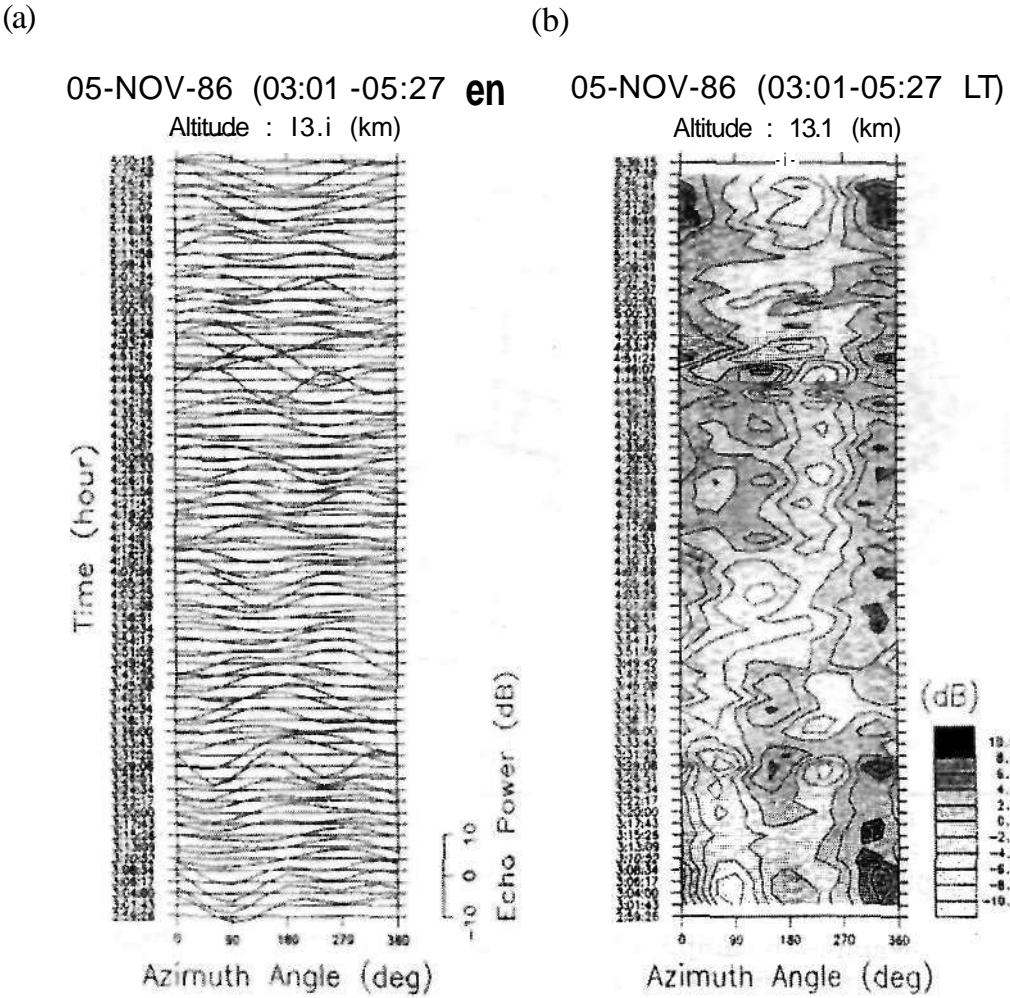


Figure 5-3: The time evolution of the azimuth angle variations of the echo power at 6° off the zenith, illustrated about every 137 second (a), and (b) a contour plot for the MU radar observations at 13.1 km.

Figure 5-4 shows an example of the amplitude and phases at 13.1 km from 03:01 to 05:27 LT on November 5, 1986. From this figure we can see that the amplitude of A_{60} and A_{jao} are comparable when double humped structure appeared during 03:17 to 03:49 LT and 04:12 to 04:49 LT as seen in Figure 5-3. This figure also indicates that A_{jeo} was generally larger than A_{iso} . Time variations of the phases were fairly smooth. Continuous progression of 0360 along time can be recognized between 03:35 and 04:05 LT, which suggests this phenomenon is caused by a propagating gravity wave.

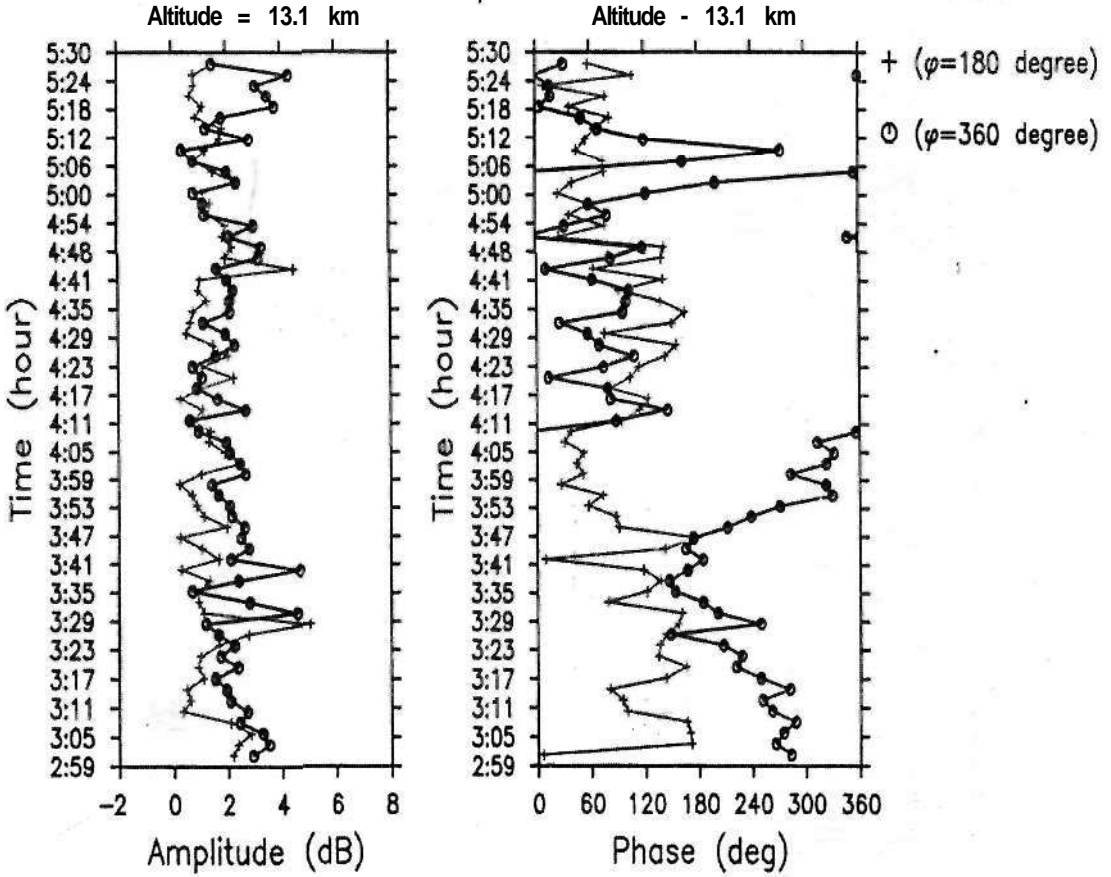


Figure 5-4: An example the amplitude and phase of echo power for observation on November 5, 1986 from 3:01 to 05:27 LT at 13.1 km. Plus and circle marks indicate for 0 180 and 360 degree, respectively

In a future study, it is required to investigate variations of wind velocity observed simultaneously with EAR in order to confirm the effects of gravity waves. In this case, we firstly present a preliminary result of EAR observation in determining zonal and meridional wind velocity variations over Kototabang from May 24-25, 2001. Then, we continue showing the long-term observation of meridional wind velocity variations from September to December 2001 as shown in Figures 6-4 to 6-6.

6 SIMULTANEOUS OBSERVATIONS WITH THE EAR AND GPS RADIOSONDE

Figure 6-1 shows time-height cross-section of zonal-meridional winds averaged every 15 min observed with the EAR from May 24-25, 2001 (20-02 LT) by Hashiguchi *et al.* (2001). In this period, tropopause height was about 16 km from the ground. Wind reversal of zonal components (namely westerly and easterly below and above 6 km, respectively) are observed. This may be associated with *Walker circulation*.

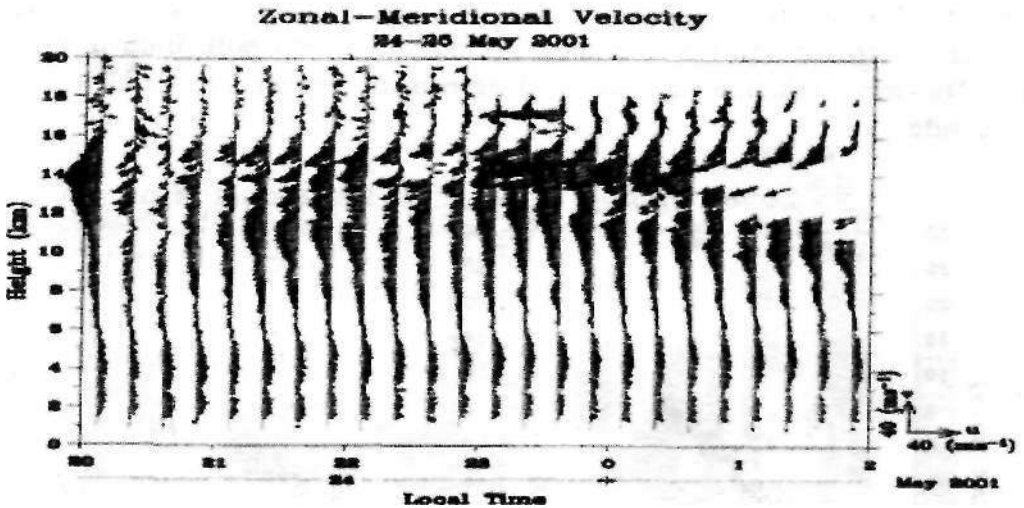


Figure 6-1: The time-height cross-section of zonal-meridional winds averaged every 15 min observed with the EAR during May 24-25, 2001 (20-02 LT) (after Hashiguchi *et al.*, 2001)

In order to evaluate the accuracy data obtained by the EAR, Hashiguchi *et al.* (2001) compared the observation data of the EAR with those of GPS radiosonde. Figure 6-2 shows the height profiles of the wind velocities obtained by the EAR averaged over 00:22-01:21 LT on May 25, 2001 and the GPS radiosonde launched near the radar side at 00:22 LT. Both wind velocities are in good agreement in the height range of 1.5-10 km and 15-20 km. The discrepancies of zonal winds at 10-15 km heights are due to low signal-to-noise (SNR) ratio of the EAR echoes.

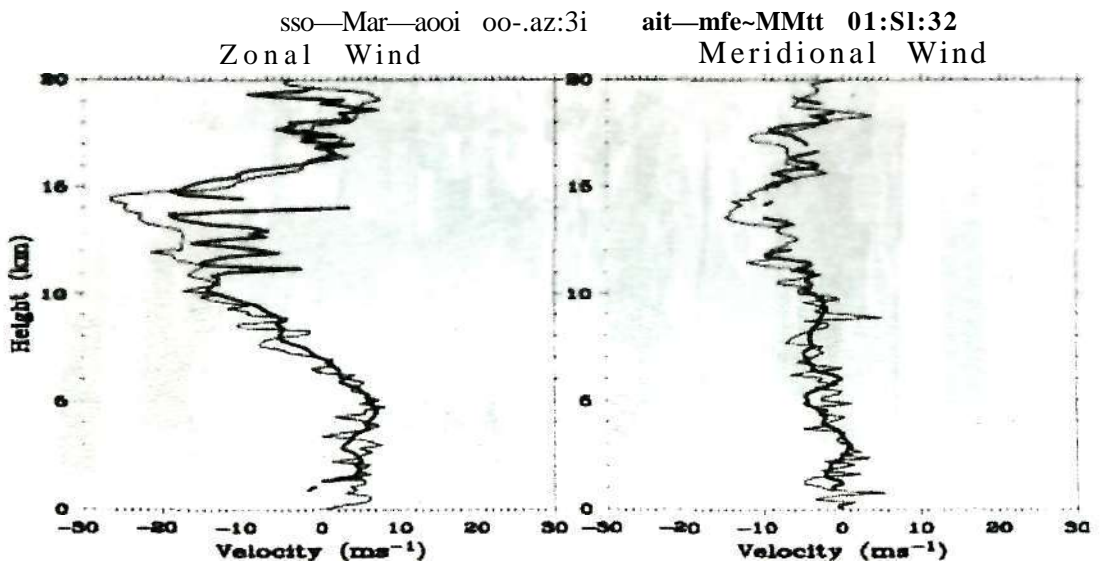


Figure 6-2: The height profiles of zonal (left panel) and meridional (right panel) winds obtained with the EAR (thick curves) averaged over 00:22-01:21 LT on May 25, 2001 and with GPS radiosonde (thin curves) launched at 00:22 LT

Figure 6-3 shows the scatter plot of horizontal winds obtained with the EAR and GPS radiosonde during May 24-25, 2001. The data in all time and in all height range, where effective data are obtained with both instruments are used. The wind velocities are in good agreement between the EAR and GPS radiosonde.

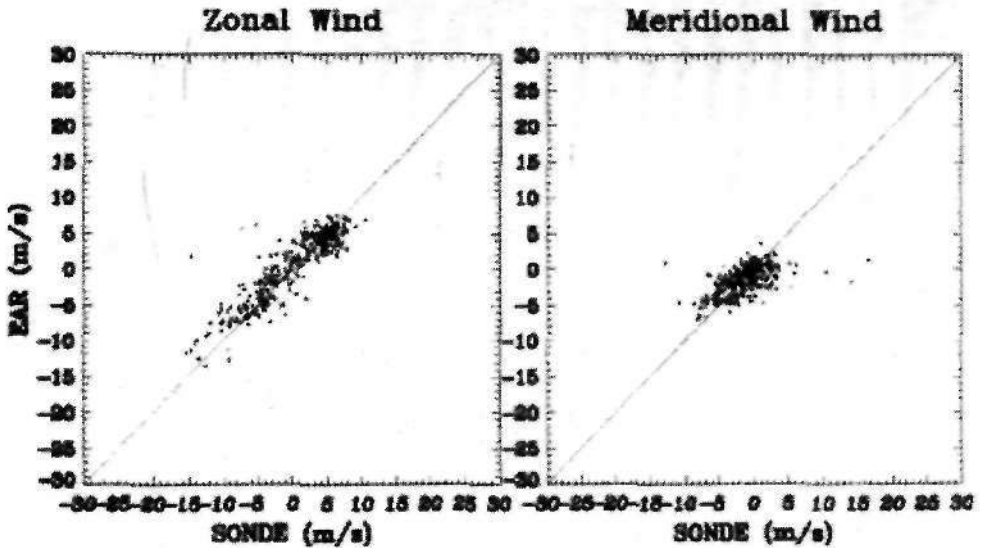


Figure 6-3: The scatter plot of zonal (left panel) and meridional (right panel) wind velocities observed with the EAR and GPS radiosonde during May 24-25, 2001

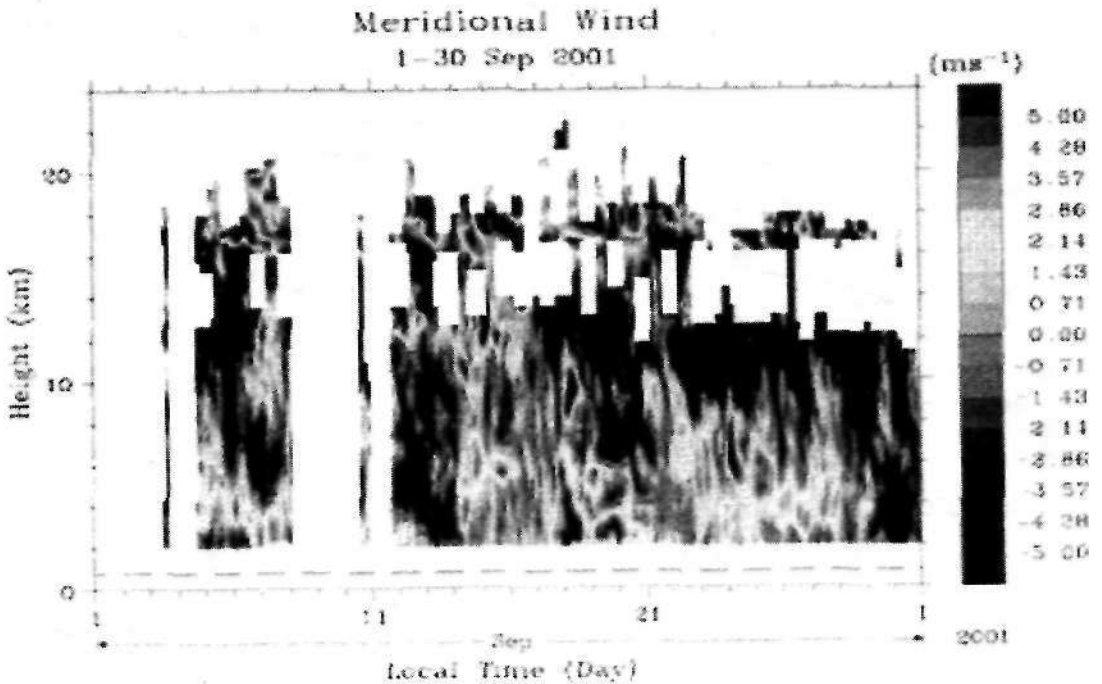


Figure 6-4: The time-height section of meridional wind velocity variations in September 2001

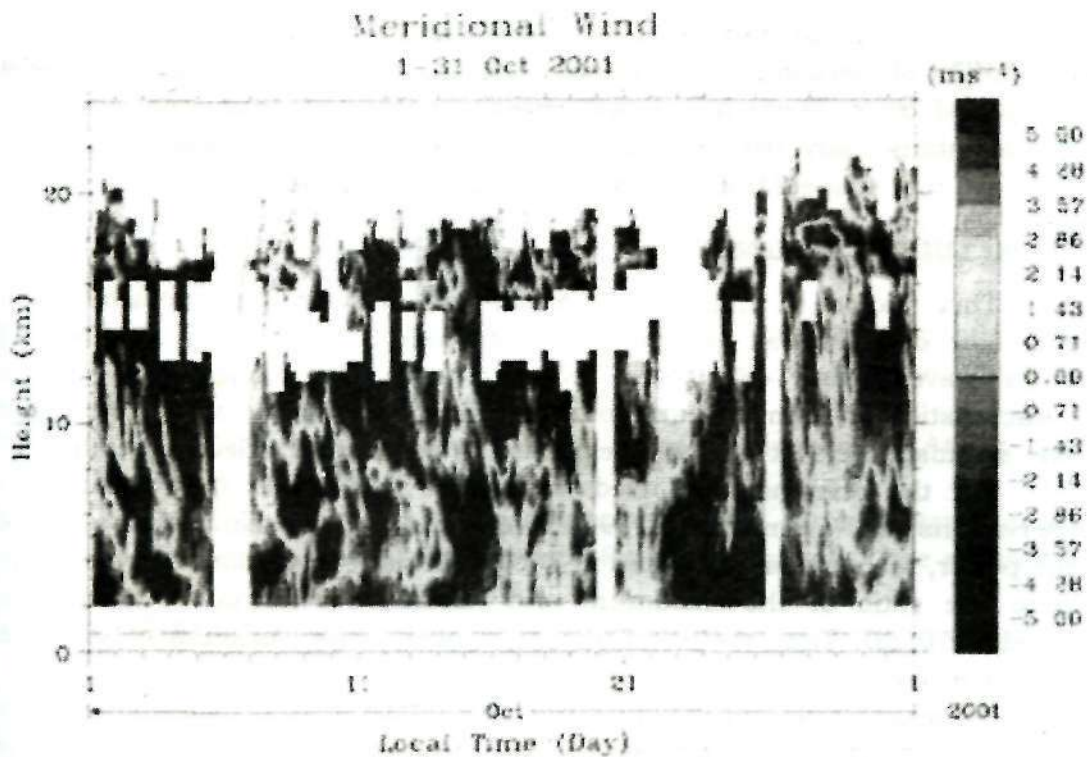


Figure 6-5: As the same as Fig. 6-4, but for October 2001

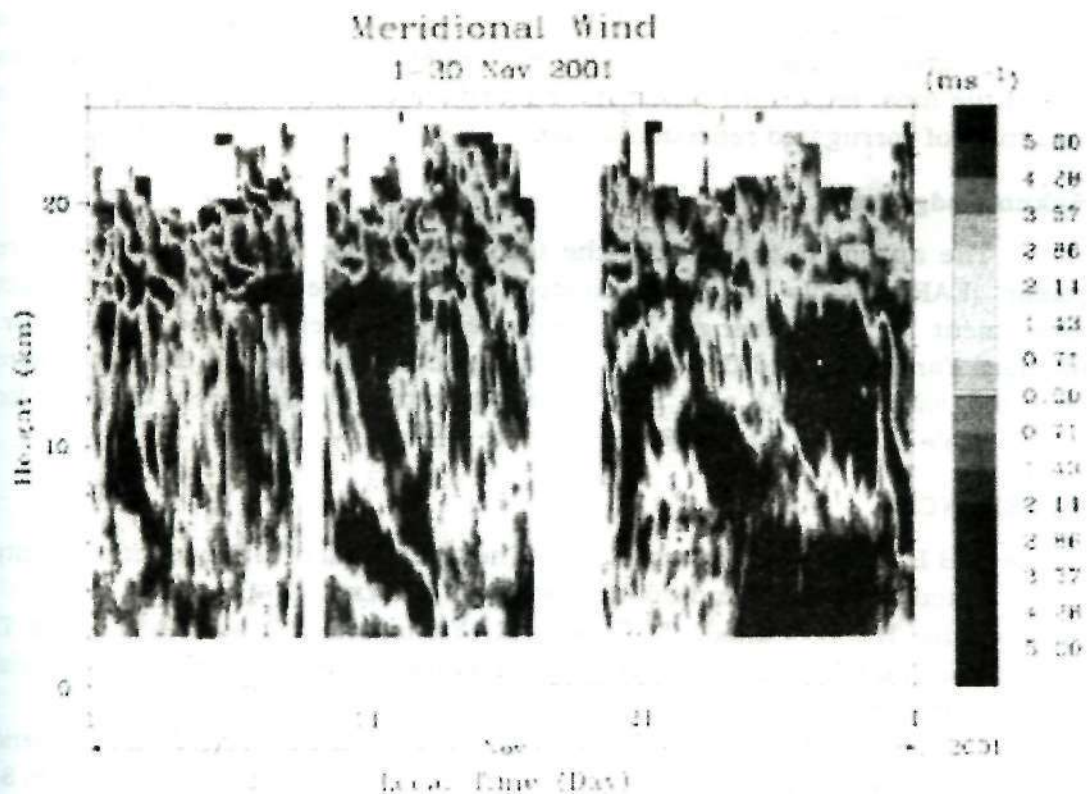


Figure 6-6: As the same as Fig. 6-4, but for November 2001

By looking at Figures 6-4 to 6-6, we can see a clear downward propagation of meridional wind velocity from 22 km to 2 km, which indicated by the *red color*. There are many waves appeared in that time. We need calculate statistically, before we mention that is caused by the effects of gravity waves. We just suspect that mostly is caused by gravity wave activities.

7 CONCLUDING REMARKS

This paper is mainly concerned an overview the possibility an application of Equatorial Atmosphere Radar (EAR) data on study the effects of gravity waves on a corrugated reflection layer. We concentrate on the characteristics of azimuth variations of echo power in the troposphere and lower stratosphere that seems to be caused by corrugated reflection surface.

For the reference, we used the Middle and Upper (MU radar) data observations on November 4-5, 1986. We found a clear azimuth variation of echo power, with one or two cycles in 360° , especially in the lower stratosphere where the ratio of the maximum and minimum echo power sometimes exceeded 10 dB. Time evolution of the azimuth angle variation of the echo power is also recognized.

Persistent time and height structures of the azimuth variations of the echo power suggest that the vertical motions caused by propagating gravity waves modify the reflection surface. As a preliminary result, we present characteristics of zonal-meridional wind velocities observed by the EAR from May 24-25, 2001 together with GPS radiosonde data. Then, we complete it this study by investigating the fluctuating components of vertical wind velocity as one of the most important parameter needed for quantitatively understand the structure of corrugated reflection surface.

Acknowledgments

The author is thankful to the technical at the Equatorial Atmosphere Radar (EAR) facility whose dedicated efforts made possible to conduct experiment at Kototabang, West Sumatera, Indonesia, especially to Dr. Mamoru Yamamoto and Dr. Hiroyuki Hashiguchi. Data used in this study were collected with the MU and EAR radar operated by Research Institute for Sustainable Humanosphere (RISH) of Kyoto University, Japan.

REFERENCES

- Balsley, B.B. and D.A. Carter, 1992. The spectrum of atmospheric velocity fluctuations at 8 and 86 km, *Geophys. Res.Lett*, 9, 465-468.
- Hashiguchi, H., S. Fukao, T. Tsuda, M. Yamamoto, T. Nakamura, and T. Horinouchi, 2001. Initial observation results with Equatorial Atmosphere Radar.
- Meek, C.E., I. M. Reid, and A.H. Manson, 1985. Observation of mesospheric wind velocities 2. Cross-sections of power spectral density for 48-8h, 8-1h, 1h-10 min over 60-100 km from 1981, *Radio Sci.*, 20, 1383-1402.

- Smith, S.A., D.C. Fritts, and T.E. VandZandt, 1985. Comparisons mesospheric wind spectra with a gravity wave model. *Radio ScL*, 20, 1331-1338.
- Tsuda, T., P.T. May, T. Sato, S. Kato, and S. Fukao, 1988. Simultaneous observations of reflection echoes and refractive index gradient in the troposphere and lower stratosphere, *Radio ScL*, 23, 655-665.
- Tsuda, T., S. Kato, T. Yokoi, T. Inoue, M. Yamamoto, T.E. VandZandt, S. Fukao and T. Sato, 1990. Gravity waves in the mesosphere observed with the MU radar, *Radio ScL*, 26, 1005-1018.
- Tsuda, T., T.E. VandZandt, and H. Saito, 1997. Zenith-angle dependence of VHF specular reflection echoes in the lower atmosphere, *J. Atmos.Terr.Phys.*, 59, 761-775.
- Vincent, R.A., 1984. Gravity wave motions in the mesosphere, *J. Atmos. Terr. Phys.*, 46, 119-128.
- Wilson, R., M.X. Chanin, and A. Hauchecorne, 1991a. Gravity waves in the middle atmosphere observed with Rayleigh lidar : 1. Case studies, *J. Geophys. Res.*, 96, 5153-5167.
- Wilson, R., M.L. Chanin, and A. Hauchecorne, 1991b. Gravity waves in the middle atmosphere observed With Rayleigh lidar : 2. Climatology, *J. Geophys. Res.*, 96, 5169-5183.